

Polymorphism of Amino Acid-Based Dendrons: From Organogels to Microcrystals

Gui-Chao Kuang,^[a] Ming-Jun Teng,^[a] Xin-Ru Jia,^{*[a]} Er-Qiang Chen,^{*[a]} and Yen Wei^[b]

Abstract: There is a delicate balance for a low-weight molecule to behave as a gelator or crystal. The synthesis of two novel amino acid-based naphthalene-dendrons, **Nap-G1** and **Nap-G2** is described. Both dendrons display polymorphic properties in organic solvents. **Nap-G1** developed a fibrous network with β -sheet architecture in cyclohex-

ane but exhibited a spherulitic network in mixed solvents (chloroform/petroleum ether 1:5, v/v). On the other hand, **Nap-G2** acted as an efficient organoge-

lator in chloroform but formed crystalline fibers in relatively high polarity solvents (such as acetone and methanol). Combinations of characterizations have been employed to study the polymorphism.

Keywords: amino acids • β sheets • dendrons • polymorphism • self-assembly

1. Introduction

The past decades have witnessed a surge of research progress dedicated to dendritic gelators owing to their advantages of tunable architectures and diverse functionalities.^[1] A number of dendritic gelators were created by using polyamide,^[2] amino acids,^[3] and poly(benzyl ether)^[4] as building blocks. The precisely controlled structures such as chirality, size, and shape show direct impact on the macroscopic gelation properties.^[1] Although the kinetic properties of gelation and the mechanism of low-molecular weight organogelators have been studied extensively, the polymorphism of dendritic gelators remains an elusive goal. Until now, many helpful ways, such as subtle change in structure,^[5] introducing cosolvents,^[6] changing supersaturation,^[7] adding additives,^[8]

and prolonging aging time,^[9] have been developed to ascertain the mechanism of gelation, however, it is still difficult to manipulate a compound to act as a gelator or a crystal clearly. Clarification of the mechanism for molecular packing in gel phase and bulk crystals of compounds also remains a challenge.^[10] A seductive strategy to understand the polymorphism is to design molecular architectures that possess large aromatic groups, including anthraquinone,^[11] anthracene,^[9] dehydrobenzoannulenes,^[12] naphthalene^[13], etc.

Gelation arises from a delicate balance of molecules that dissolve or self-assemble in selective solvents, depending on the interactions between gelator–gelator and gelator–solvent.^[10] It has been previously seen that the solvent-mediated intermolecular interactions play a critical role in the formation of gels or crystals. In fact, the solvent diversity may contribute to the complexity of gelation by three means: 1) efficient gelation would occur by controlling gelator–solvent interactions to a proper hydrophobic and hydrophilic balance; 2) the formation of a 3D network requested for gelation would be prohibited if crystal growth and branching are unfavorable in a selected solvent; 3) complicated gel morphologies would be observed owing to the internal structures and polarity of solvents.^[14] Very recently, studies investigating the impact of introducing different solvents on morphology have been reported.^[6] For example, Liu and co-workers described the transition from dipeptide-based gel phase to flower-like microcrystal by adding ethanol as a cosolvent to toluene.^[6a] Wan and co-workers demonstrated the sugar-appended gel to crystal transition by changing the ratios of the mixed solvents of water/1,4-dioxane.^[6b]

[a] Dr. G.-C. Kuang, M.-J. Teng, Prof. X.-R. Jia, Prof. Dr. E.-Q. Chen
Beijing National Laboratory for Molecular Sciences
and Key Laboratory of Polymer Chemistry
and Physics of the Ministry of Education
College of Chemistry and Molecular Engineering
Peking University
Beijing, 100871 (China)
Fax: (+86) 10-6275-1708
E-mail: xrjia@pku.edu.cn
eqchen@pku.edu.cn

[b] Prof. Dr. Y. Wei
Department of Chemistry
Tsinghua University
Beijing, 100084 (China)

Supporting information for this article is available on the WWW under <http://dx.doi.org/10.1002/asia.201000529>.

Previously, we have reported a series of dendrons based on amino acids that not only acted as efficient organogelators but also showed liquid-crystalline properties.^[15] Motivated by the important role that underlying solvents play in dendritic gelators, we prepared two novel dendrons **Nap-G1** and **Nap-G2** by using aspartic acid (Asp) and alanine (Ala) as the building block and naphthalene as the focal group. Though possessing quite similar structures, both display quite different polymorphic architectures in the solvents with different polarity. **Nap-G1** self-assembled into a fibrous network with β -sheet architecture in cyclohexane but exhibited spherulitic-network morphology in the mixed solvents (chloroform/petroleum ether 1:5, v/v). In contrast, **Nap-G2** acted as an efficient organogelator in chloroform but showed crystalline fibers in higher polarity solvents such as acetone and alcohol. We demonstrate that in both dendrons the naphthyl group plays a crucial role for additional driving forces to form polymorphic architecture. Very recent observations, that introduce the bulk aromatic group at the N terminal contribute to the complexation of self-assembly described by Adam et al., are consistent with our postulation on naphthyl producing polymorphism.^[5]

2. Gelation Properties

Nap-G1 and **Nap-G2** gels were prepared by a sonication method. In brief, a certain amount of the compound was dissolved in an organic solvent, and then the solution was subjected to the ultrasound for a sufficient time. Whether the gel could be obtained after the sonication was dependent on the amount of gelator and the solvents used.^[16] The behavior of the dendrons in various solvents is listed in Table 1. Both **Nap-G1** and **Nap-G2** display good solubility in dimethyl sulfoxide (DMSO) and *N,N*-dimethyl formamide (DMF). **Nap-G1** demonstrates its gelation properties in nonpolar solvents such as cyclohexane, decane, and petroleum ether, whereas **Nap-G2** precipitates in these liquids. When the sol-

Table 1. Gelation behavior of **Nap-G1** and **Nap-G2** in the common solvents at 25°C.

Solvents	Nap-G1		Nap-G2	
	CGC ^[a]	T_{gel} ^[b]	CGC ^[a]	T_{gel} ^[b]
Decane	G(1.1)	98°C	P	n.d.
Petroleum ether	G(1.0)	65°C	P	n.d.
Cyclohexane	G(0.4)	83°C	P	n.d.
Ethyl acetate	S	n.d.	G(1.4)	90°C
Chloroform	S	n.d.	G(0.5)	59°C
Acetone	S	n.d.	VF	n.d.
Methanol	S	n.d.	VF	n.d.
Ethanol	S	n.d.	VF	n.d.
DMF	S	n.d.	S	n.d.
DMSO	S	n.d.	S	n.d.

[a] G, P, VF, and S denote gelation, precipitation, viscous fluid, and solution, respectively. The critical gelation concentration (CGC, wt%) is shown in parentheses and S represents no gelation formed below 100 mg mL⁻¹. [b] The diameter of the vial is 10 mm and the heating rate is 1°C min⁻¹ in an oil bath. n.d. = not determined.

vents were changed to polar solvents, such as chloroform and ethyl acetate, **Nap-G2** acts as an efficient gelator. However, only the viscous fluids were observed when **Nap-G2** was dissolved in the solvents with higher polarity such as acetone, ethanol, and methanol. Conversely, **Nap-G1** showed good solubility in these polar solvents. This obvious difference in gelation behavior indicates that **Nap-G2** is a more polar compound owing to more amide fragments included in its branches. Meanwhile, the gel transition temperature (T_{gel}) was determined when the stable gel, inverted in a thermostated oil bath, changed to a fluid-like solution (i.e., fell under the gravity influence). The results demonstrate that solvents have a direct impact on the gel stability (Table 1).

Nap-G1 can form an opaque gel with cyclohexane at a concentration above 0.4 wt% (Figure 1a). Transmission electron microscopy (TEM)^[17] images reveal that most of

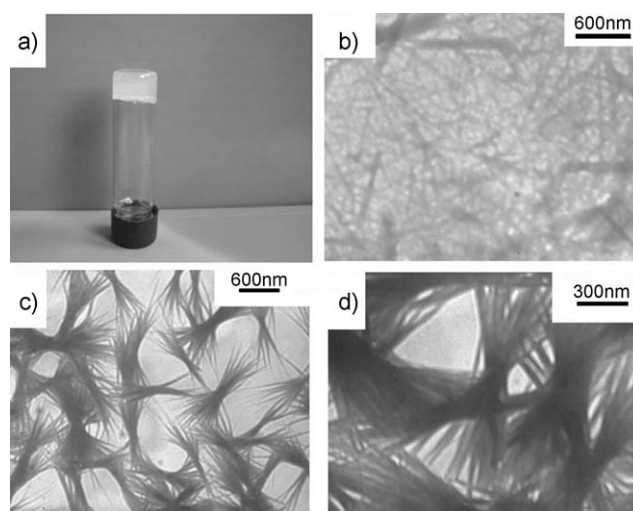


Figure 1. a) Picture of a gel of **Nap-G1**/cyclohexane; b) TEM image of xerogel **Nap-G1**/cyclohexane on a copper grid covered with Formvar film; c) and d) TEM image of **Nap-G1** xerogel obtained from the mixed solvent of chloroform/petroleum ether (1:5, v/v) with different magnifications.

the interconnected straight fibers are hundreds of nanometers long and approximately 40 nm wide (Figure 1b). In comparison, to form fibrous assemblies in cyclohexane, **Nap-G1** gel displays a spherulitic-network morphology in the mixed solvent of chloroform/petroleum ether (v/v = 1:5) with the needle-like fibers growing from the typical “permanent junction zones” (Figure 1c, d). Such spherulitic-morphology development may involve the following three steps: 1) the fiber branches initiated from a nucleation center; 2) highly branched fibers radially grew from the central nucleation site; and 3) ultimately the branches impinged on or entangled each other to shape the 3D networks.^[18] The network formation process can probably be considered as a continuous fibers growth-branching process. The final evolution diagram is demonstrated in Figure 1. If the fiber growth overwhelms the branching, a fiber network with a large

aspect ratio (the length over the width) will form (Figure 1b). In the opposite case, a spherulitic-morphology network will develop (Figure 1c, 1d).

Nap-G2 gel could be prepared immediately in chloroform under sonication, and the gel became more and more opaque after aging for several hours (see Figure S4 in the Supporting Information). The fast gel formation may be attributed to the ultrasound triggering, which probably accelerated the fibrous aggregation of the gelators. The more opaque gel appearance could be the result of either further development of the fibers or the transition from gel phase to crystal after extended aging time. TEM images of **Nap-G2** xerogel reveal the intertwined nanobelts with a large aspect ratio. The average width of the nanobelts is around 100 nm (Figure 2a and b), much wider than that of the

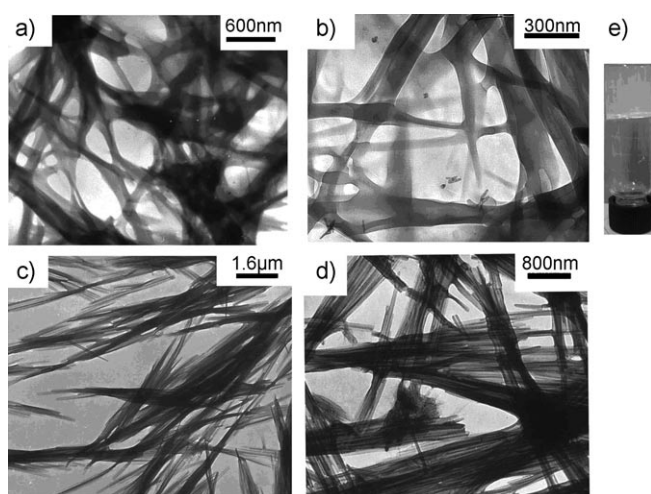


Figure 2. a) and b) TEM images of **Nap-G2**/chloroform xerogel on copper grid covered with Formvar film at different magnifications; c) and d) TEM images of **Nap-G2** crystals from acetone on a copper grid with different magnifications; e) gel picture of **Nap-G2**/chloroform.

fibers of dendrons (glycine and aspartic acid as building blocks) reported in our previous papers.^[15] This might be mainly due to the different focal functional groups. Although the dendrons based on amino acids bear the similar dendritic portion, the stronger aromatic stacking between the naphthyl groups may enhance the extent of interdigitation, thereby leading to widening of the nanobelts.^[19] Figure 2c and 2d show the TEM images of microbelts obtained from the viscous fluid of **Nap-G2**/acetone. The magnified image (Figure 2d) depicts the microbelts, which are shown to be much thinner compared to that shown in Figure 2a. The different aggregate morphologies of **Nap-G2** in chloroform and acetone reflect the influence of the polarity of solvents. It is clear that the microbelt aggregates from acetone showed almost no branch off, which leads to the viscous fluid but not the gel.

3. Polymorphic Structure Analysis

The superstructure of **Nap-G1** in cyclohexane was investigated by FTIR, Circular dichroism (CD), ¹H NMR spectroscopy, 2D nuclear Overhauser effect spectroscopy (NOESY), and wide-angle X-ray diffraction (WAXD). We found that the **Nap-G1**/cyclohexane gel was highly related to the β -sheet structure. Xu and co-workers^[20] and Ulijn and co-workers^[21] have studied some aromatic short-peptide derivatives that are capable of forming hydrogels. They demonstrate that the β -sheet packing is a key structure for the gel-phase assemblies. For **Nap-G1** in chloroform, the solution shows the characteristic FTIR absorption bands at 3438 (ν_{N-H}), 1660 (amide I, $\nu_{C=O}$), and 1521 (amide II , δ_{N-H} ; Figure 3a). However, these bands shift to 3227, 1634, and 1535 cm^{-1} in the gel phase of **Nap-G1**/cyclohexane, thus in-

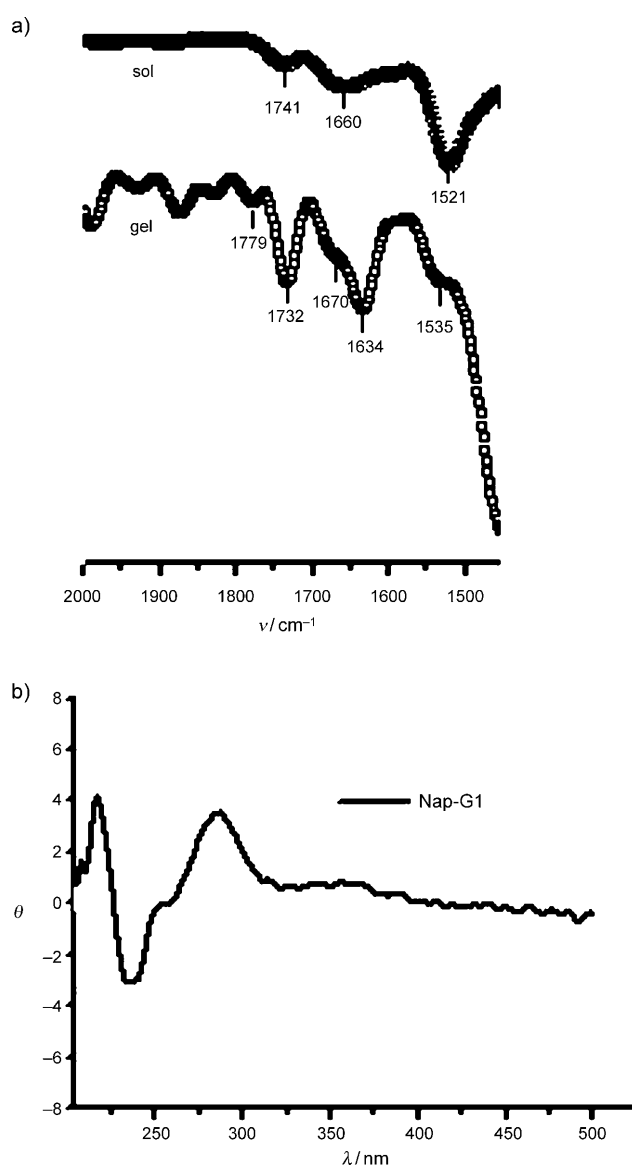


Figure 3. a) FTIR spectra of **Nap-G1** in a chloroform solution and in the gel of cyclohexane; b) CD spectrum of **Nap-G1**/cyclohexane gel.

dicating the presence of an antiparallel β -sheet (instead of parallel) arrangement in the aggregates (Figure 3a). In the CD spectrum of **Nap-G1**/cyclohexane gel (Figure 3b), two positive Cotton effects near 215 and 285 nm, which can be attributed to π - π^* transition of the phenyl and naphthyl aromatics, respectively, are observed. Moreover, a negative Cotton effect at 230 nm is ascribed to π - π transition of the phenyl group. These results are consistent with the β -sheet conformation of the amide bond.^[22] The concentration-dependent ^1H NMR spectroscopic experiments of **Nap-G1** in deuterated chloroform (CDCl_3) were performed to further understand the intermolecular hydrogen-bonding interaction of **Nap-G1** (Figure 4a, b). With the concentration up to 50 mg mL^{-1} , **Nap-G1**/ CDCl_3 remained as a clear solution. The proton signal at 6.47 ppm (3 mg mL^{-1}) can be assigned to the amide group of **Nap-G1**, which gradually shifts downfield with increasing **Nap-G1** concentration, and this reflects formation of the hydrogen bonds. However, the 2D NOESY spectrum indicates the development of intermolecular hydrogen bonds between the two amide groups of **Nap-G1** is not suffi-

cient in chloroform. As shown in Figure 4b, the additional cross-peak generated by the intermolecular interaction between N-H and the methine proton H^* was confirmed (Scheme 1). Therefore, the shifted proton should be only ascribed to the amide located near the naphthyl group. In this case, **Nap-G1** cannot form an ordered structure (e.g., β sheet) in chloroform solution through self-assembly.

The WAXD^[23] results further supported the β -sheet architecture of **Nap-G1** in cyclohexane. As shown in Figure 5a, the xerogel of **Nap-G1**/cyclohexane can render the diffractions up to the seventh order, with their scattering vector ratio of 1:2:3:5:6:7. This indicates that the xerogel possesses a lamellar structure with the first-order diffraction corresponding to a layer period of 32.6 \AA . Furthermore, we can observe an additional diffraction at 4.3 \AA in the wide-angle region, which can be ascribed to the spacing between peptides within the β -sheet structure.^[24] According to calculations from the CPK model, the size (from the focal point to the periphery) of **Nap-G1** is estimated to be about 18.8 \AA with the assumption that **Nap-G1** is in a fully extended

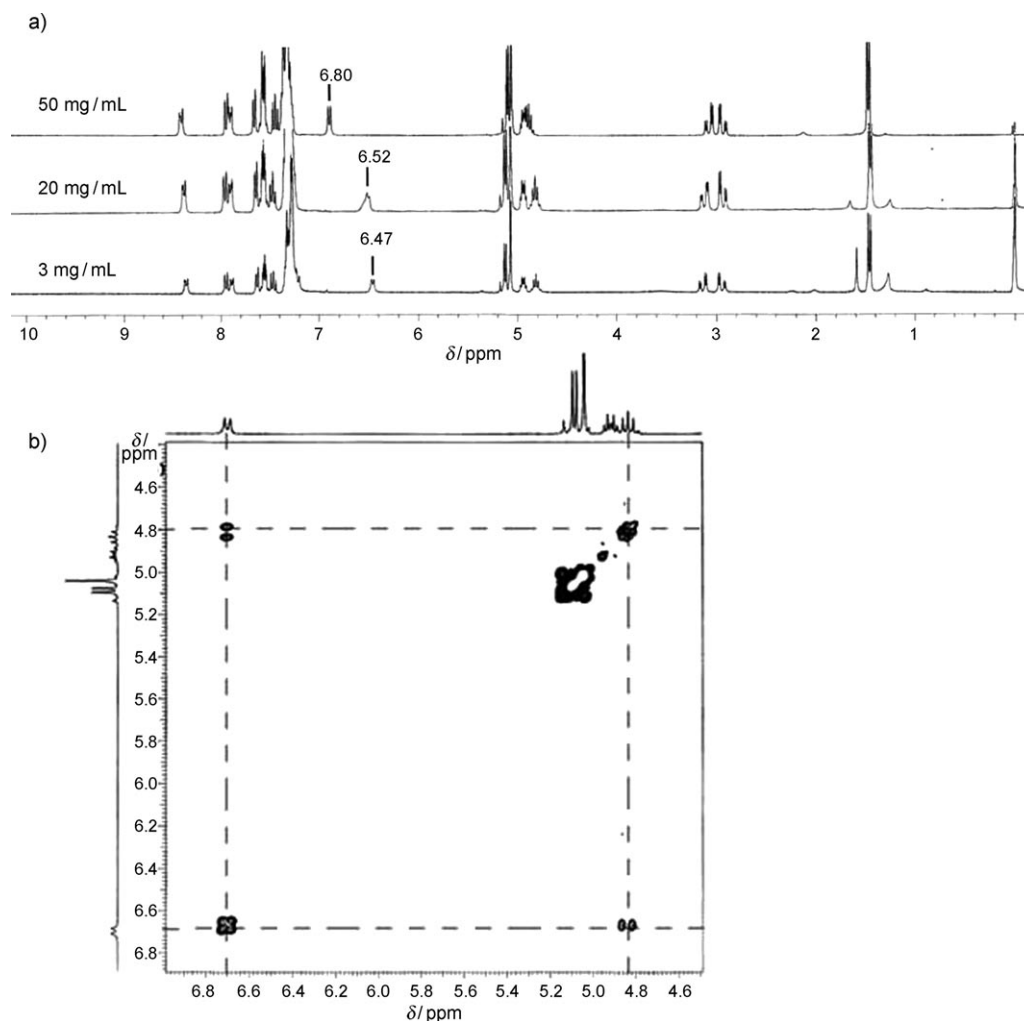
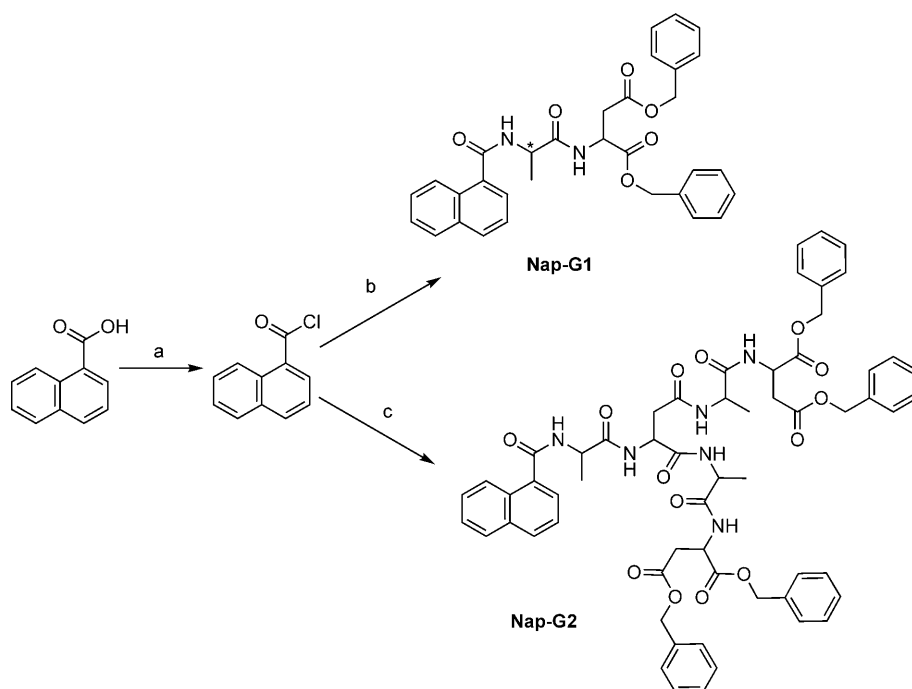


Figure 4. a) ^1H NMR spectra of **Nap-G1** in chloroform at different concentrations and recorded at 25°C ; b) portions of the NOESY spectrum of 50 mg mL^{-1} in chloroform at 25°C .



Scheme 1. Structures of **Nap-G1** and **Nap-G2**. a) SOCl_2 , reflux, 2 h; b) $\text{CF}_3\text{COO-G1}$, triethylamine, CHCl_3 , RT, 24 h; c) $\text{CF}_3\text{COO-G2}$, triethylamine, CHCl_3 , RT, 24 h. For synthetic details, see the Supporting Information.

state. Hence, each lamella might consist of two layers of **Nap-G1**, in which the naphthyl groups are partially interdigitated with the benzyl groups. This packing fashion may provide an additional driving force for the self-assembly of **Nap-G1**.^[20] Figure 5b depicts a schematic model of the molecular packing. As the lamellar period is smaller than twice the extended molecular length of **Nap-G1**, interdigitated bilayers are easily formed through intermolecular hydrogen bonding and π - π stacking interactions.

As shown in Figure 1, **Nap-G1** xerogel obtained from the mixed solvent of chloroform/petroleum ether (1:5, v/v) presents the spherulitic network, which is drastically different from that of **Nap-G1**/cyclohexane. This implies that the molecular packing would also be different. The diffraction pattern of **Nap-G1**/mixed-solvent xerogel exhibits a set of well-resolved diffraction peaks (Figure 6), thereby indicating a crystalline structure with an order higher than the lamellar packing of **Nap-G1** in cyclohexane. The first-order diffraction centered at $2\theta = 3.4^\circ$ corresponds to a d spacing of 2.6 nm, which is smaller than the layer period of the interdigitated β -sheet structure but is still much larger than the size of the **Nap-G1** with an extended conformation. As the WAXD powder pattern lacks dimensionality, the crystalline structure cannot be solved at this moment. It is also intriguing to observe that the solvent with relatively high polarity can completely inhibit the ordered packing of **Nap-G1**. In Figure 6, the WAXD pattern from a powder sample obtained after drying the **Nap-G1**/ CHCl_3 solution only shows an amorphous halo in the low-angle region, the center (at around $2\theta = 5.8^\circ$) of which corresponds to a dimension of 1.5 nm, which is close to the molecular size of **Nap-G1**. In

this case, we presume that the molecules are trapped in an amorphous state, which might be ascribed to the fast evaporation of chloroform.

The solvents also played a critical role in the self-assembly of **Nap-G2**. The high solution viscosity of **Nap-G2** in acetone and alcohols shall arise from the long microbelts that intercross each other. We found that slow evaporation of the solvent could lead the microbelts to settle at the bottom of the cuvette, thus forming a piece of dry white sheet with the long axis of microbelts parallel to the sheet surface. The sheet could be employed to run the 2D WAXD test in two orthogonal directions (see the insets of Figure 7a and b, wherein the x direction is parallel to the sheet surface and the z direction is the normal surface). Fig-

ure 7a and b depict the 2D WAXD patterns of a sheet sample obtained from **Nap-G2**/acetone with the X-ray incident beam perpendicular and parallel to the z direction, respectively. The ring pattern of Figure 7b indicates that the ordered domains within the sheet are rotationally disordered around the z direction. On the other hand, Figure 7a reveals the orientation of the sample. On the basis of the diffraction geometry, we assume that the diffraction arcs along the z direction can be attributed to $(hk0)$, whereas those along the x direction are $(00L)$. The detailed indices of the integral-intensity profile of the 2D WAXD patterns are shown in Figure 7c (see also Table S1 in the Supporting Information). This indexing corresponds to an orthorhombic cell with $a = 3.05$ nm, $b = 2.66$ nm, and $c = 0.83$ nm. In this case, it is very possible that the **Nap-G2** molecules form columns that pack parallel to form a 2D centered rectangular structure. Previously,^[15c] we have shown that a dendritic gelator with an azo group at the focal point formed a similar type of architecture, which has also been described by Jang and Aida^[25] and Percec^[26] in their study on dendritic molecules. The density of the **Nap-G2** sample was measured to be 1.30 g cm^{-3} . With the value of the c axis of 0.83 nm, a calculation based on the method by Percec et al.,^[26] we determined that the number of the molecules located in each column in the rectangular unit cell is 2.4. Figure 7d shows the WAXD powder pattern of the **Nap-G2**/chloroform xerogel. It can be seen that some strong diffractions of the xerogel peak at similar positions appear in Figure 7c; however, some diffractions (particularly those in the high-angle region) are much broader, indicating that the packing of the molecules are less perfect. Moreover, we can observe two

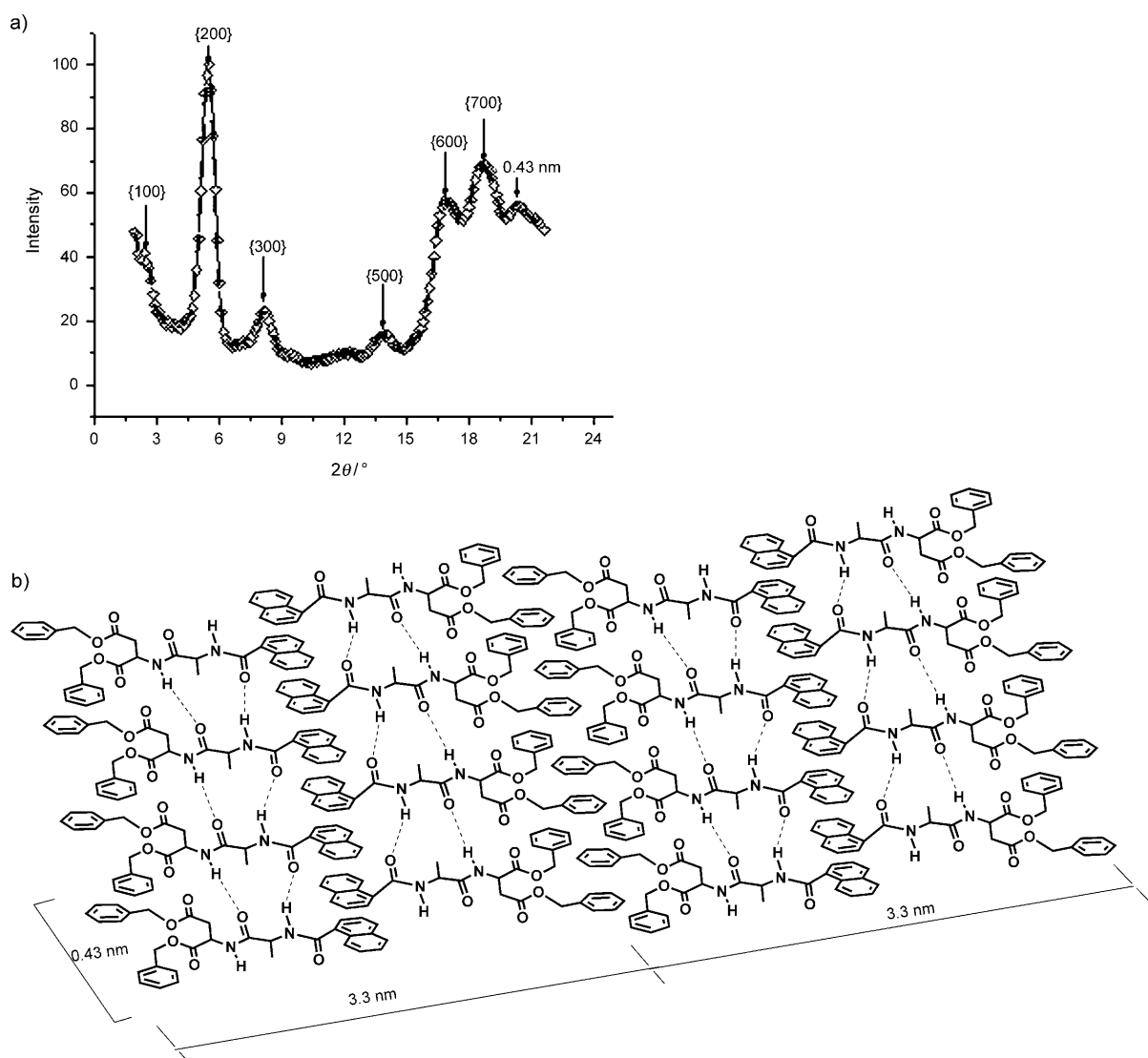


Figure 5. a) WAXD pattern of **Nap-G1** xerogel made from cyclohexane; b) the proposed bimolecular-layer model for gelation.

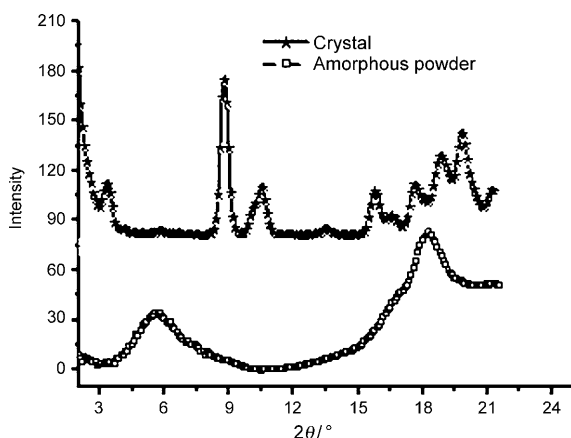


Figure 6. WAXD patterns of **Nap-G1** xerogel from the mixed solvent of chloroform/petroleum ether (1:5, v/v) and amorphous powder obtained from drying the chloroform solution.

new diffractions at 2θ lower than 5 degrees. This infers that the molecular packing in xerogel is different from the orthorhombic structure of **Nap-G2** in viscous fluid, or the xerogel of **Nap-G2**/chloroform may contain a mixed structure.

4. Conclusions

We have investigated polymorphic properties of two naphthyl-dendrons **Nap-G1** and **Nap-G2** in selective solvents. Our results demonstrate that **Nap-G1** formed a gel in cyclohexane with β -sheet architecture but exhibited spherulitic-network morphology in the mixed solvents such as chloroform/petroleum ether (1:5, v/v). **Nap-G2** in chloroform self-organized into intertwined nanobelts, acting as an efficient organogelator. On the other hand, in high-polarity solvents of acetone and alcohols, it formed crystal microbelts with an orthorhombic structure. To the best of our knowledge, this

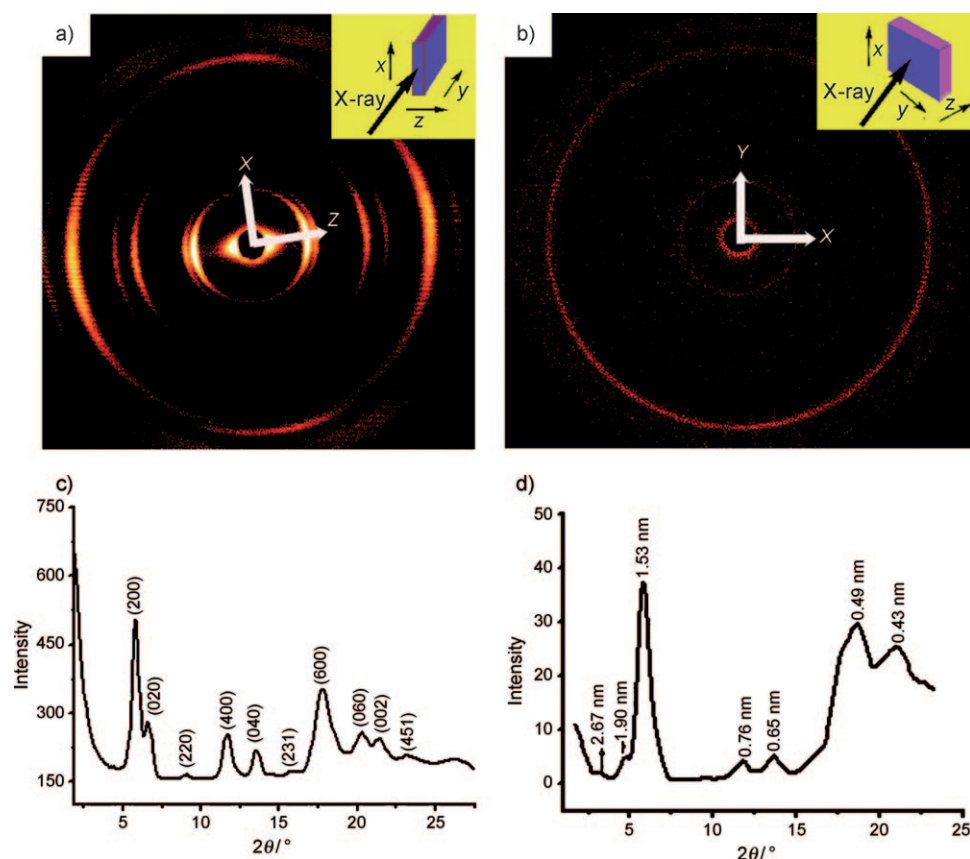


Figure 7. a) and b) 2D WAXD patterns of the sheet sample of **Nap-G2** obtained after drying the acetone solution slowly in air. The insets show the sample orientation with respect to the X-ray incident beam. *x* and *z* directions are parallel and perpendicular to the sheet surface, respectively; c) integral-intensity profile of the WAXD pattern shown in (a). The peaks are indexed with an assumed orthorhombic structure of **Nap-G2** crystal; d) WAXD powder pattern of **Nap-G2**/chloroform xerogel.

is the first report referring to the polymorphism of the self-assembly of dendrons in selective solvents. These results might provide a broad perspective for the design of novel self-assembly architectures.

Experimental Section

5. Gel Preparation

Samples for gelation studies were prepared by ultrasound (200 W) in 10 mm (i.d.) vials sealed at one end. For example, **Nap-G1** (3 mg) and cyclohexane (1 mL) were added to the vial sequentially. The sealed vial was sonicated at room temperature. Gelation was determined by the absence of flow of the solvent when the tube was inverted. Critical gel concentration was determined by weighing up a minimum amount of gelator needed for the stable gel formation.

6. Materials and Measurements

All reagents and organic solvents were obtained from commercial sources and were used as received except when specified otherwise. The synthesis and characterization of the dendrons are described in the Supporting Information.

^1H NMR spectra were recorded on Bruker 400 MHz spectrometers at room temperature using $[\text{D}_6]$ DMSO and/or CDCl_3 as the solvent and tetramethylsilane as an internal standard. ^{13}C NMR spectra were recorded

on Bruker 100 MHz spectrometers. Matrix-assisted laser desorption/ionization time-of-flight (MALDI-TOF) mass spectra were acquired on a BIFLE XIII time-of-flight MALDI mass spectrometer with α -cyano-4-hydroxycinnamic acid (CCA) as the matrix, which gives the best resolution. FTIR spectra were obtained by using a Bruker VECTOR22 IR spectrometer. CD spectra of the gels and solutions were recorded on a Jasco J-810 spectropolarimeter equipped with a Julabo F25 thermostatic apparatus. The samples were dropped into or prepared in a quartz cuvette with a path length of approximately 1 mm. The fluorescence emission measurements were carried out at room temperature in chloroform by using a Hitachi F-4500 fluorescence spectrophotometer. Transmission electron microscopy (TEM) experiments were performed by using a JEM-100 CXII microscope with an acceleration voltage of 100 kV. Wide-angle X-ray diffraction (WAXD) patterns of xerogels were obtained by using a Bruker D8 Discover diffractometer with GADDS as a 2D detector. The diffraction patterns were recorded in transmission mode at room temperature by employing $\text{Cu}_{\text{K}\alpha}$ radiation. The background scattering was recorded and then subtracted. The gel samples were naturally dried for two days at room temperature before WAXD experiments.

Acknowledgements

This work is supported by the National Natural Science Foundation of China (NSFC No. 20774003 and 20974004 to X. R. Jia and No. 20774006 to E. Q. Chen).

- [1] D. K. Smith, *Adv. Mater.* **2006**, *18*, 2773.
- [2] C. Kim, K. T. Kim, Y. Chang, *J. Am. Chem. Soc.* **2001**, *123*, 5586.
- [3] a) H. F. Chow, J. Zhang, *Chem. Eur. J.* **2005**, *11*, 5817; b) H. F. Chow, J. Zhang, *Tetrahedron* **2005**, *61*, 11279.
- [4] a) M. Seo, J. H. Kim, J. Kim, N. Park, J. Park, S. Y. Kim, *Chem. Eur. J.* **2010**, *16*, 2427; b) W. D. Jang, D. L. Jiang, T. Aida, *J. Am. Chem. Soc.* **2000**, *122*, 3232; c) V. Percec, M. Peterca, M. E. Yurchenko, J. G. Rudick, P. A. Heiney, *Chem. Eur. J.* **2008**, *14*, 909; d) M. Yoshida, Z. M. Fresco, S. Ohnishi, J. M. J. Fréchet, *Macromolecules* **2005**, *38*, 334; e) Y. Feng, Z. T. Liu, J. Liu, Y. M. He, Q. Y. Zheng, Q. H. Fan, *J. Am. Chem. Soc.* **2009**, *131*, 7950.
- [5] D. J. Adams, K. Morris, L. Chen, L. C. Serpell, J. Bacsá, G. M. Day, *Soft Matter* **2010**, *6*, 4144.
- [6] a) P. L. Zhu, X. H. Yan, Y. Su, Y. Yang, J. B. Li, *Chem. Eur. J.* **2010**, *16*, 3176; b) J. X. Cui, Z. H. Shen, X. H. Wan, *Langmuir* **2010**, *26*, 97.
- [7] R. Y. Wang, X. Y. Liu, J. Y. Xiong, J. L. Li, *J. Phys. Chem. B* **2006**, *110*, 7275.

- [8] a) S. H. Tung, Y. E. Huang, S. R. Raghavan, *Soft Matter* **2008**, *4*, 1086; b) X. Y. Liu, P. D. Sawant, *Angew. Chem.* **2002**, *114*, 3793; *Angew. Chem. Int. Ed.* **2002**, *41*, 3641.
- [9] a) X. Huang, P. Terech, S. R. Raghavan, R. G. Weiss, *J. Am. Chem. Soc.* **2005**, *127*, 4336; b) X. Huang, S. R. Raghavan, P. Terech, R. G. Weiss, *J. Am. Chem. Soc.* **2006**, *128*, 15341.
- [10] a) P. Dastidar, *Chem. Soc. Rev.* **2008**, *37*, 2699; b) X. Y. Liu, *Top. Curr. Chem.* **2005**, *256*, 1.
- [11] a) P. Terech, E. Ostuni, R. G. Weiss, *J. Phys. Chem.* **1996**, *100*, 3759; b) P. Terech, G. Clavier, H. B. Laurent, J. P. Desvergne, B. Demé, J. L. Pozzo, *J. Colloid Interface Sci.* **2006**, *302*, 633; c) Y. G. Li, Y. Fang, J. Liu, M. Z. Wang, *J. Chin. Chem. Soc.* **2006**, *53*, 359; d) G. M. Clavier, J. F. Brugger, H. Bouas-Laurent, J. L. Pozzo, *J. Chem. Soc. Perkin Trans. 2* **1998**, 2527.
- [12] I. Hisaki, H. Shigemitsu, Y. Sakamoto, Y. Hasegawa, Y. Okajima, K. Nakano, N. Tohnai, M. Miyata, *Angew. Chem.* **2009**, *121*, 5573; *Angew. Chem. Int. Ed.* **2009**, *48*, 5465.
- [13] Z. M. Yang, G. L. Liang, B. Xu, *Chem. Commun.* **2006**, 738.
- [14] a) S. Yagai, M. Ishii, T. Karatsu, A. Kitamura, *Angew. Chem.* **2007**, *119*, 8151; *Angew. Chem. Int. Ed.* **2007**, *46*, 8005; b) G. Y. Zhu, G. S. Dordick, *Chem. Mater.* **2006**, *18*, 5988.
- [15] a) Y. Ji, Y. F. Luo, X. R. Jia, E. Q. Chen, Y. Huang, C. Ye, B. B. Wang, Q. F. Zhou, Y. Wei, *Angew. Chem.* **2005**, *117*, 6179; *Angew. Chem. Int. Ed.* **2005**, *44*, 6025; b) W. S. Li, X. R. Jia, B. B. Wang, Y. Ji, Y. Wei, *Tetrahedron* **2007**, *63*, 8794; c) Y. Ji, G. C. Kuang, X. R. Jia, E. Q. Chen, B. B. Wang, W. S. Li, Y. Wei, J. Lei, *Chem. Commun.* **2007**, 4233; d) G. C. Kuang, Y. Ji, X. R. Jia, Y. Li, E. Q. Chen, Y. Wei, *Chem. Mater.* **2008**, *20*, 4173; e) G. C. Kuang, Y. Ji, X. R. Jia, E. Q. Chen, M. Gao, J. M. Yeh, Y. Wei, *Chem. Mater.* **2009**, *21*, 456.
- [16] Y. G. Li, T. Y. Wang, M. H. Liu, *Tetrahedron* **2007**, *63*, 7468.
- [17] The dried gel sample for TEM measurement was obtained by exposing the wet gel to air for two days, the evaporation of solvent may exert a significantly negative influence on gel formation due to the high vacuum for TEM analysis (Ref. [7]). We examined the structure of gelators in the solid state with an assumption that the molecular packing in the gel state might be reflected by it.
- [18] R. Y. Wang, X. Y. Liu, J. Narayanan, J. Y. Xiong, J. L. Li, *J. Phys. Chem. B* **2006**, *110*, 25797.
- [19] a) Z. M. Yang, B. Xu, *Chem. Commun.* **2004**, 2424; b) K. Balakrishnan, A. Datar, T. Naddo, J. Huang, R. Oitker, M. Yen, J. Zhao, L. Zang, *J. Am. Chem. Soc.* **2006**, *128*, 7390.
- [20] Z. M. Yang, B. Xu, *J. Mater. Chem.* **2007**, *17*, 2385 and the references therein.
- [21] a) R. V. Ulijn, A. M. Smith, *Chem. Soc. Rev.* **2008**, *37*, 664; b) A. M. Smith, R. J. Williams, C. Tang, P. Coppo, R. F. Collins, M. L. Turner, A. Saiani, R. V. Ulijn, *Adv. Mater.* **2008**, *20*, 37.
- [22] a) N. Sreerama, R. W. Woody, *Circular Dichroism: Principles and Applications* (Eds.: N. Berova, K. Nakanishi, R. W. Woody), Wiley, New York, **2000**, pp. 601; b) Z. M. Yang, G. L. Liang, L. Wang, B. Xu, *J. Am. Chem. Soc.* **2006**, *128*, 3038.
- [23] The XRD method developed by Weiss and co-workers (see Ref. [9]) is suitable for characterization of the arrangement of some gelators, but a lot of other gels fail to give significant signals. We have tried to monitor the molecular pattern of the gel phase of **Nap-G2** in situ by XRD, but failed to get any useful information. **Nap-G2** gel (please see Figure 2c and Figure S4 in the Supporting Information) prepared in chloroform displayed strong scattering under X-ray. For the gel prepared in other solvents, no significant signals were obtained owing to the low concentration of the gelator (~1 wt %).
- [24] a) Y. Matsuzawa, K. Ueki, M. Yoshida, N. Tamaoki, T. Nakamura, H. Sakai, M. Abe, *Adv. Funct. Mater.* **2007**, *17*, 1507; b) T. Miyazawa, E. R. Blout, *J. Am. Chem. Soc.* **1961**, *83*, 712; c) S. Matsumura, S. Uemura, H. Mihara, *Chem. Eur. J.* **2004**, *10*, 2789; d) A. Aggeli, M. Bell, L. M. Carrick, C. W. G. Fishwick, R. Harding, P. J. Mawer, S. E. Radford, A. E. Strong, N. Boden, *J. Am. Chem. Soc.* **2003**, *125*, 9619.
- [25] W. D. Jang, T. Aida, *Macromolecules* **2003**, *36*, 8461.
- [26] a) V. Percec, M. Glodde, T. K. Bera, Y. Miura, I. Shiyonovskaya, K. D. Singer, V. S. K. Balagurusamy, P. A. Heiney, I. Schnell, A. Rapp, H. W. Spiess, S. D. Hudson, H. Duan, *Nature* **2002**, *417*, 384; b) V. Percec, C. M. Mitchell, W. D. Cho, S. Uchida, M. Glodde, G. Ungar, X. B. Zeng, Y. S. Liu, V. S. K. Balagurusamy, P. A. Heiney, *J. Am. Chem. Soc.* **2004**, *126*, 6078.

Received: August 2, 2010

Published online: February 24, 2011